PHYSICAL REVIEW E **69**, 015301(R) (2004)

Oscillatory axial banding of particles suspended in a rotating fluid

G. Seiden,[1] S. G. Lipson,[1,*] and J. Franklin[2]
[1]*Department of Physics, Technion-Israel Institute of Technology, 32000 Haifa, Israel*
[2]*Department of Physics, Temple University, Philadelphia, Pennsylvania 19122, USA*
(Received 8 April 2003; published 28 January 2004)

A nonviscous fluid, completely filling a tube rotating about its horizontal axis, contains a suspension of macroscopic particles. The particles are observed to distribute themselves spontaneously in bands distributed periodically along the axis, with a band separation dependent only on the tube radius and length. In many cases, the bands oscillate periodically between two interleaving patterns. We explain this banding phenomenon as arising from the excitation of inertial standing waves in the rotating fluid.

DOI: 10.1103/PhysRevE.69.015301 PACS number(s): 47.55.Kf, 47.35.+i, 47.54.+r

In a recent paper, Lee and Ladd [1] described the axial banding of non-Brownian particles suspended in a rotating viscous fluid at Reynolds number $\mathrm{Re} \ll 1$. Their geometry involved a cylindrical tube of radius R, completely filled with fluid, rotating about a horizontal axis with angular velocity Ω. A mechanism involving a balance between gravitational, viscous, and centrifugal forces was shown to cause the particles to segregate into axial bands with separation Λ independent of Ω, the viscosity of the fluid, and the geometry of the particles. For two types of boundary conditions at the tube walls, band separations of $\Lambda = 1.8R$ and $3.9R$ were found; these were compared with experiments by Matson *et al.* [2] on suspensions of 100 μm silica particles in glycerol solutions, for which $\Lambda \approx 2.6R$. Axial banding of larger particles in completely filled rotating tubes of less viscous fluids with $\mathrm{Re} \gg 1$ has also been reported recently [3–5], with values of Λ between 3.5 and $4R$.

In this paper, we present an experimental study and an explanation of the banding of much larger particles in rotating fluids of negligible viscosity, with Re of order 100–300. An example is shown in Fig. 1. Previous observations [4,5] on the same system showed that the banding is independent of Ω and occurs for a wide range of particle types and sizes. In contrast to the predictions of Lee and Ladd [1], banding was also observed for negatively buoyant particles, i.e., air bubbles. The experiments reported here were carried out in glass tubes of internal radii R between 12.8 and 22.9 mm, rotating with $\Omega \sim 6$ rad/sec. This rotation is fast enough to lift the particles off the bottom of the tube (or top, in the case of bubbles), but not large enough to centrifuge them to the wall. Otherwise, its precise value does not seem to be important. The length of the tube was varied by means of a teflon piston. The tubes were completely filled with water or dilute glycerol solutions. Monodisperse collections of nylon, polystyrene, and plexiglass particles, air bubbles and polydisperse dendritic crystals were suspended in the rotating fluid. A minimum number of about ten particles per band was necessary for banding to occur; otherwise the particles did not occupy preferential positions along the tube. Increasing the viscosity by up to 20% in dilute glycerol solutions was found to have no effect on the results. In some cases with crystals and bubbles, the bands were very narrow and well defined [4].

The experiments were photographed and recorded on video tape for subsequent analysis. Figure 1 shows the bands formed by plexiglass cylinders with a band forming at one end of the tube, but not at the other. In general, the end could either be at the center of a band or halfway between two bands, there being no observable preference between the two cases. This resulted in the existence of two degenerate interleaved patterns for each value of L. When bubbles were present together with particles, bubble bands interleaved with particle bands. In addition, we found a different oscillatory phenomenon in which the bands alternated periodically between the two possible patterns. An example of this oscillatory behavior is shown in Fig. 2.

The band spacings Λ were measured as a function of the tube length L after the photographs had been digitized. The results for a large number of experiments using different types of particles and tubes are shown in Fig. 3, in which Λ/R is plotted as a function of L/R. Particles of different types, indicated on the figure by different symbols, all lie on the same universal plot, consisting of a set of straight lines represented by $L = n\Lambda/2$, where $n = 2,3 \ldots$. This appears similar to other standing wave phenomena; except that for odd n, bands occur at one end or the other as in Fig. 1, whereas for even n, the bands occur either at both ends or at neither, as in Fig. 2. This suggests the bands to be at intervals of Λ, not the usual $\Lambda/2$, which will be explained by the theoretical analysis. It can also be seen in Fig. 3 that Λ increases linearly with L until a limiting value of about $L = 4R$ is reached, at which point it jumps to the next value of n. Oscillations between the two different patterns (Fig. 2)

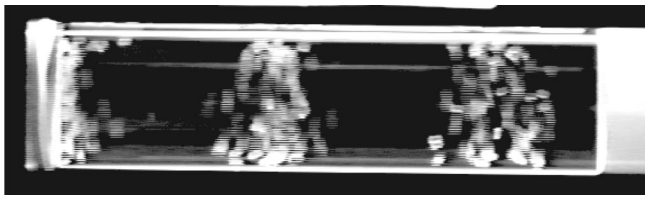

FIG. 1. Example of bands formed by 220 plexiglass cylinders at a rotation rate $\Omega = 9.4$ rad/sec in a 2.57 cm diameter tube 11.2 cm long. Notice that there is a band at the end of the tube on the left, but the right end is half a period distant from the nearest band.

*Electronic address: sglipson@physics.technion.ac.il

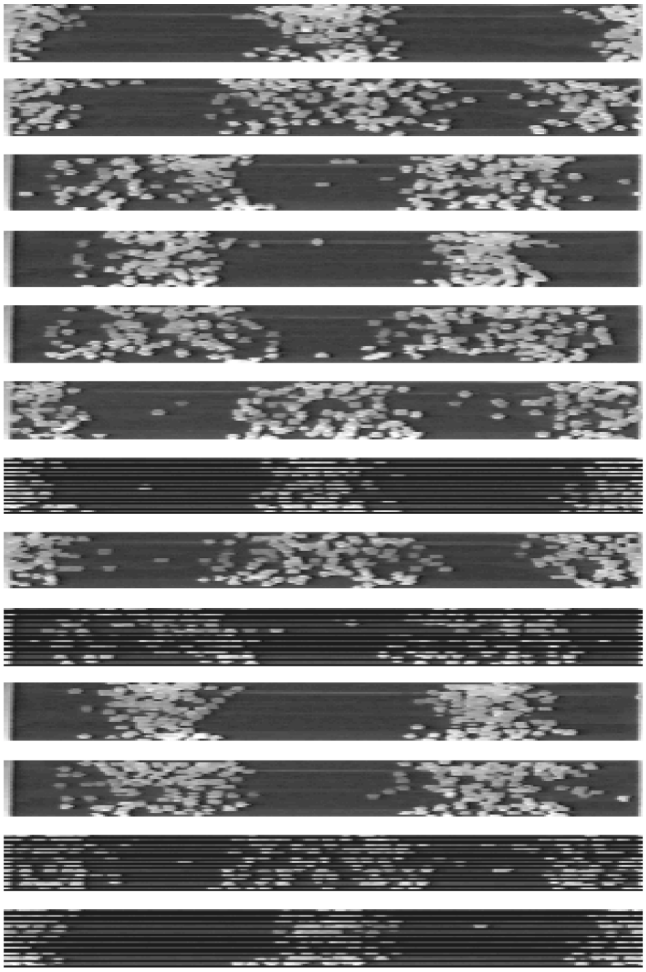

FIG. 2. Pictures of the bands at time intervals of 3.5 sec to illustrate the oscillation phenomenon, with 3 mm polystyrene balls in a tube of diameter 4.45 cm at $\Omega = 5.5$ rad/sec.

were observed in many cases, with periods in the range 10–30 sec.

Experiments were also carried out in which both individual motion and collective particle motion were observed from the end of the tube. In the case of a single particle, an off-center neutral point on the x axis was found where it could remain in equilibrium between the drag forces and gravity, or around which stable circulation took place. We note that this equilibrium point was shown by Lee and Ladd [1] to be unstable in the low Re regime, but particles would remain there for long periods. In the many-particle case, when the bands formed, the particles moved within a fairly well-defined torus around the neutral point, as can be seen in Fig. 4(a). Their angular velocity, measured by timing selected painted particles, was found to be in the range 0.95–1.00 Ω. However, during oscillations between modes the simple rotary motion of the particles ceased, as in Fig. 4(b). At the same time, we could observe the particle motion from the side and see that the particles developed an organized roll-like motion in which they appeared to be repelled from the band at the bottom of the falling part of the cycle, and return to join it during the rising part. This type of motion can also be discerned in the illustrations in Ref. [2].

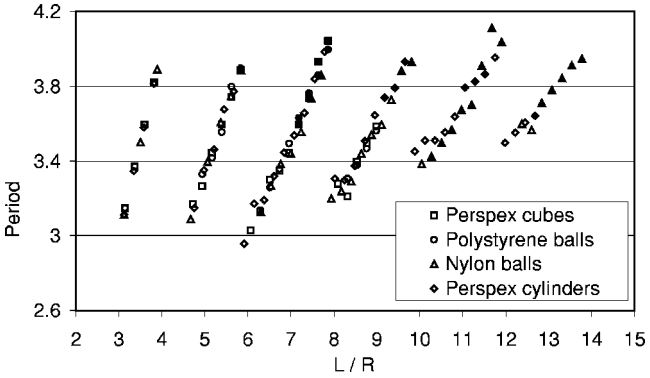

FIG. 3. Dependence of the band separation on the length of the tube, scaled to the tube radius. The different types of particle are indicated by different symbols. The filled symbols indicate oscillating states.

During the oscillations, particles from adjacent bands meet at the midpoint where they form a new band.

The observations in Fig. 3 show that a standing wave phenomenon is involved, so that although the mechanism proposed by Lee and Ladd [1] might be involved in initially promoting banding, it cannot be dominant since the amplification peak at $\lambda = 3.8R$ is too broad to support a single-mode type of behavior [6]. Instead, we suggest that interaction between the particles and the rotating fluid excites resonant inertial waves in the fluid [7,8] whose frequency ω is close to or equal to Ω. The particles then accumulate in axial regions where the combined flow pattern of rotating fluid and wave is most consistent with the normal rotational motion resulting from the drag of the rotating fluid and the downward force of gravity.

Current interest in inertial waves is mainly limited to geophysical and atmospheric physics [9], although the basic ideas have been known for 120 years [7]. In the frame of reference rotating with angular velocity $\mathbf{\Omega}$ (where the main body of the fluid is at rest), the Navier-Stokes equations are

$$\nabla \cdot (\rho \mathbf{v}) = -\frac{\partial \rho}{\partial t}, \tag{1}$$

$$\frac{\partial(\rho \mathbf{v})}{\partial t} + \mathbf{v} \cdot \nabla(\rho \mathbf{v}) + 2\mathbf{\Omega} \times \rho \mathbf{v} + \mathbf{\Omega} \times (\mathbf{\Omega} \times \rho \mathbf{r}) = -\nabla p + \rho \mathbf{g} + \mathbf{F}. \tag{2}$$

In this equation, the pressure p and the velocity $\mathbf{v}$ represent perturbations to the rigid-body motion of the rotating fluid. The vector $\mathbf{g}$ is the gravitational acceleration, which rotates at angular velocity $-\mathbf{\Omega}$ in the rotating system. $\mathbf{F}$ represents a driving force per unit volume due to the action of the suspended particles on the fluid.

We simplify Eq. (2) by introducing a new pressure variable $\overline{p}$ including the effect of the centrifugal and gravitational forces,

$$\overline{p} = p - \tfrac{1}{2}\rho(\mathbf{\Omega} \times \mathbf{r})^2 - \rho \mathbf{g} \cdot \mathbf{r}. \tag{3}$$

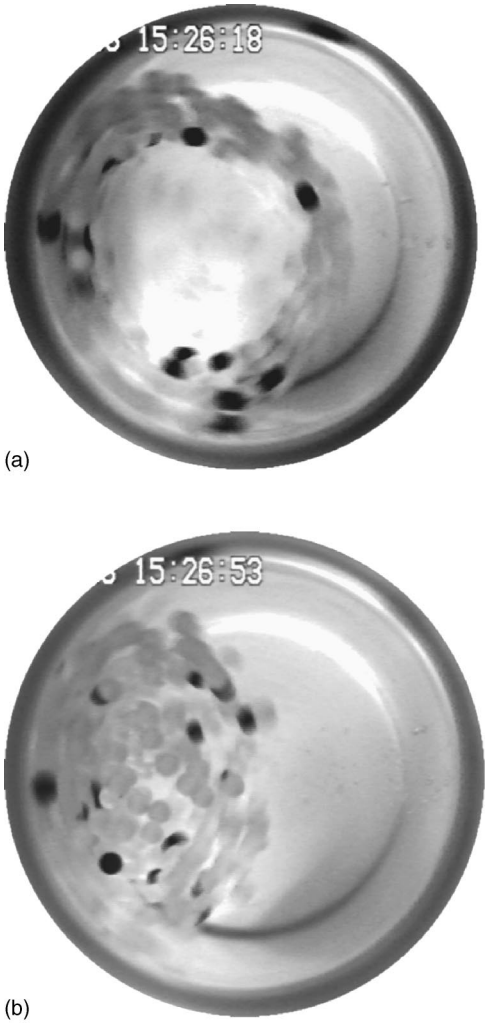

FIG. 4. Photographs of particle distributions as seen from the end of a 5.58 cm diameter tube during oscillations: (a) when the bands are clearest, (b) when the bands are mixed (least clear). Several balls were painted black in order to measure the rotation speed. Rotation is in the clockwise sense.

We further assume the fluid, generally water, to be incompressible and linearize the problem by dropping the nonlinear $\mathbf{v}\cdot\boldsymbol{\nabla}(\rho\mathbf{v})$ term. These steps reduce Eq. (2) to

$$\frac{\partial(\rho\mathbf{v})}{\partial t}+2\boldsymbol{\Omega}\times\rho\mathbf{v}=-\boldsymbol{\nabla}\overline{p}+\mathbf{F}. \tag{4}$$

In the rotating system, F drives the system with a time dependence $\sim e^{-i\omega t}$. Eliminating the vector $\rho\mathbf{v}$ from Eqs. (1) and (4), and taking the time dependence $e^{-i\omega t}$ for $\overline{p}$, we get a wave equation for $\overline{p}$. In cylindrical coordinates r,θ,z, this equation is

$$\frac{1}{r}\frac{\partial}{\partial r}\left(r\frac{\partial\overline{p}}{\partial r}\right)+\frac{1}{r^2}\frac{\partial^2\overline{p}}{\partial\theta^2}+\left(1-\frac{4\Omega^2}{\omega^2}\right)\frac{\partial^2\overline{p}}{\partial z^2}=f(\mathbf{F}), \tag{5}$$

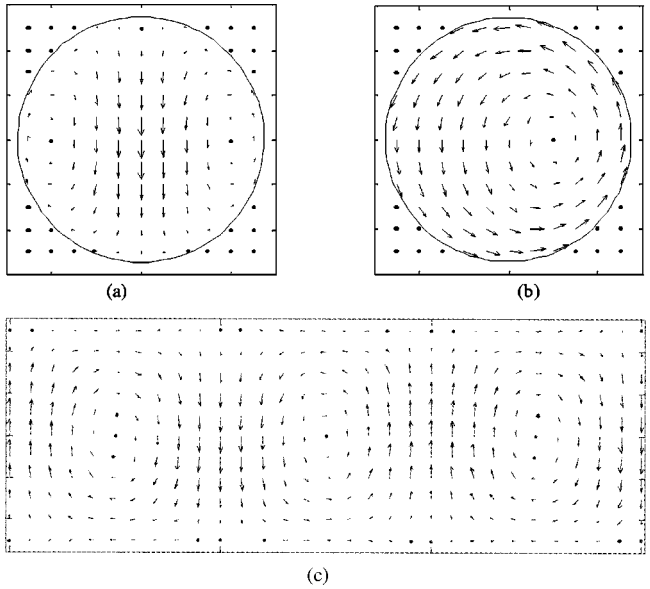

FIG. 5. Properties of the $m=-1$ inertial wave in the lab frame: (a) The wave induced velocity $\mathbf{v}$ in the plane $z=\pi/k$. (b) The total velocity $\mathbf{V}=\mathbf{v}+\boldsymbol{\Omega}\times\mathbf{r}$ in the plane $z=\pi/k$. (c) The velocity $\mathbf{V}$ in the plane $x=0$.

where $f(\mathbf{F})$ is a function of the driving force. For boundary conditions $\hat{\mathbf{n}}\cdot\mathbf{v}=0$ at the ends and curved surface ($r=R$) of the cylinder, Eq. (5) can lead to standing wave solutions.

When $\omega=\Omega$, the resonant solutions of the homogeneous equation (5) without the driving term are

$$\overline{p}=p_0J_m(\gamma r)\cos(m\theta-\Omega t)\cos kz, \tag{6}$$

where $k=\gamma/\sqrt{3}$. However, inclusion of the driving term would be expected to alter this relationship.

The appropriate value of the azimuthal number m for a gravity-driven experiment is $m=-1$, since then the pattern of the pressure wave in the rotating system will rotate with angular velocity Ω in a direction opposite to the rotation of the cylinder. In the laboratory system, this pattern would appear fixed when looked at from the end of the rotating tube. That is, the off-center fixed point of the rotating particles in Fig. 4(a) remains still.

From Eqs. (1), (4), and (6), the velocity components v_r, v_θ, v_z can be found

$$v_r=V_0\left[J_1'(\gamma r)+\frac{2J_1(\gamma r)}{\gamma r}\right]\sin(\theta+\Omega t)\cos kz, \tag{7}$$

$$v_\theta=V_0\left[2J_1'(\gamma r)+\frac{J_1(\gamma r)}{\gamma r}\right]\cos(\theta+\Omega t)\cos kz, \tag{8}$$

$$v_z=\frac{\gamma}{k}V_0\,J_1(\gamma r)\sin(\theta+\Omega t)\sin kz, \tag{9}$$

in which $V_0\equiv k^2p_0/\gamma\rho\Omega$. At $z=0,L$ the boundary conditions are $v_z=0$, giving $k=n\pi/L$ and wavelength $\lambda=2L/n$. At the curved surface of the cylinder $v_r=0$ at $r=R$, giving the eigenvalue equation

$$J_1'(\gamma R) = -2J_1(\gamma R)/(\gamma R). \quad (10)$$

The first solution is $\gamma R = 2.74$, which leads to a wavelength for the resonant waves $\lambda = 2\pi/k = 2\pi\sqrt{3}/\gamma = 3.97R$.

In the nonrotating laboratory frame, the pressure and velocity of the wave field are given by Eqs. (6)–(9) without the Ωt term in the angular dependence. The flow geometry in the cross section $z = \pi/k$ of the tube is shown in Fig. 5(a). It consists of a flow generally in the vertical direction with v_y maximum at $r = 0$. For even kz/π the velocity is upwards, while for odd kz/π, it is downwards. Figure 5(b) shows the flow pattern in the laboratory frame, where this velocity has been added to the rotational velocity $\mathbf{\Omega} \times \mathbf{r}$. We see that the result is a counterclockwise circulation about an off-center point $(x_s, 0)$, where $x_s > 0$ (< 0) in the planes where kz/π is odd (even). The longitudinal flow v_z is maximum in the regions near the walls, and has opposite directions at top and bottom as shown in Fig. 5(c). This pattern repeats periodically along the z axis, reversing sense every half wavelength $\lambda/2$. The requirement that the flow pattern match the gravity-induced particle motion determines that the particles stabilize around alternate nodal planes, where $x_s > 0$, and determines the actual value of V_0. Bubbles stabilize in the planes where $x_s < 0$. We have thus identified the banding period Λ that we observe in the experiment with the wavelength λ, and not with $\lambda/2$ as in an ordinary standing wave. Changing the sign of V_0 provides an alternative degenerate solution in which ''even'' and ''odd'' are interchanged. The oscillations between the modes presumably result from coupling between them, which so far we have ignored.

The situation described above in which $\Lambda = 3.97R \approx 4R$ is for the resonant case, where no driving term is present. This is the upper limit of the curves shown in Fig. 3. Although we do not have a solution for the wave equation with a driving term, the general effect of a driving term on k for a given $\gamma = 2.74/R$ will be to increase k. We can appreciate the effect of drag of the suspended particles by considering a simplified force $\mathbf{F} = -\alpha\rho\mathbf{v}$ on the right-hand side of Eq. (4). To lowest order in α, this modifies the resonance condition to

$$\gamma^2 = \left[\left(\frac{4\Omega^2}{\Omega^2 + \alpha^2} \right) - 1 \right] k^2; \quad (11)$$

when the tube length L is decreased below its value for resonance, the drag on the fluid causes k to become larger than $\gamma/\sqrt{3}$, thus decreasing the band separation Λ as in Fig. 3.

In summary, the physical picture which emerges is that a standing inertial wave is excited by the reactive buoyant force exerted by the gravity-driven particles on the rotating fluid. The velocity field of the excited wave, when added to the rigid-body rotation of the fluid, leads to a velocity field that couples to the natural motion of a single particle in alternate nodes of the wave. This explains the fact that, for a given tube length, there are two degenerate standing wave patterns with band separation having a maximum value $\Lambda \sim 4R$, with the extraordinary pattern of skipped nodes, although the mechanism of the oscillations between them is not clear.

We acknowledge useful discussions with Oded Regev and Amos Ori, and the technical assistance of Shmuel Hoida. One of us (J.F.) wishes to thank the Technion Physics Department for its kind hospitality during the completion of this work. The work was supported by the Minerva Center for Non-linear Science and Technion Fund for Promotion of Research.

[1] J. Lee and A.J.C. Ladd, Phys. Rev. Lett. **89**, 104301 (2002).
[2] W.R. Matson, B.J. Ackerson, and P. Tong, Phys. Rev. E **67**, 050301 (2003).
[3] A.P.J. Breu, C.A. Kreulle, and I. Rehberg, Europhys. Lett. **62**, 491 (2003).
[4] S.G. Lipson, J. Phys.: Condens. Matter **13**, 5001 (2001).
[5] S.G. Lipson and G. Seiden, Physica A **314**, 272 (2002).
[6] A. Yariv, *Optical Electronics in Modern Communications*, 5th ed. (Oxford University Press, New York, 1997).
[7] G.K. Batchelor, *An Introduction to Fluid Dynamics* (Cambridge University Press, Cambridge, 1973).
[8] H.P. Greenspan *Theory of Rotating Fluids* (Cambridge University Press, Cambridge, 1969), reprinted (Breukelen Press, Brookline, 1990).
[9] L.R.M. Maas, J. Fluid Mech. **437**, 13 (2001).